PHYSICAL REVIEW A **88**, 012304 (2013)

Off-resonant Raman-echo quantum memory for inhomogeneously broadened atoms in a cavity

S. A. Moiseev*

Kazan Physical-Technical Institute of the Russian Academy of Sciences, Russia

(Received 12 March 2013; published 8 July 2013)

A scheme of photon echo-based quantum memory in the optimal optical QED cavity with off-resonant Raman atomic transition is proposed. The scheme employs the atomic ensembles characterized by an optically thin resonant transition and natural inhomogeneous broadening of the resonant line composed of the arbitrary narrow homogeneous spectral components. The scheme provides robust and quite simple coherent control of the light atoms dynamics that can be implemented by using an existing optical technique and opens a practical way for realization of the efficient long-lived multimode optical quantum memory.

DOI: 10.1103/PhysRevA.88.012304 PACS number(s): 03.67.Ac, 42.50.Ct, 42.50.Md, 42.50.Pq

I. INTRODUCTION

Realization of efficient multimode quantum memory (QM) is a topical problem of quantum optics and quantum information science. There are a number of proposals which have provided a large progress in the last decade [1–4]; however, a simultaneous realization of main requirements such as almost ideal quantum efficiency and fidelity and long-lived and multimode capacity of QM is still the subject of intensive investigations (present state of art in the optical quantum memory based on multiatomic ensembles are presented in a special issue devoted to quantum memory, see comments in [5] and other papers in this issue). Photon echo-based QM [6] is one of the promising techniques where most successful experimental results have demonstrated the efficient quantum storage of multimode light fields in a free propagation scheme with controlled reversible inhomogeneous broadening (CRIB) realized via switching of the external electric (or magnetic) field gradients [7,8] [known as a gradient echo memory (GEM)]. However, the potentially acceptable properties of this technique have their limitations in a maximum value of controlled inhomogeneous broadening (IB) and in the realization of ultimately narrow homogeneous broadening. Therefore these two factors limit the multimode capacity, atomic decoherence, and optical depth on the resonant atomic transition. In order to resolve these problems, approaches have been proposed later such as the photon echo technique QM on the IB line composed of the periodic atomic frequency combs (AFC protocol) [9], which has been successfully demonstrated for broadband [10,11] and multimode storage [12,13] (see also the modified AFC scheme [14] providing theoretically almost 100% quantum efficiency for the broadband light fields and a QM scheme based on broadband slow light in AFC media [15]). However, a sufficiently high quantum efficiency can be realized only for rather narrow AFCs, which remains a serious experimental problem. There are other proposals of the photon or spin echo-based QMs, in particular using the natural IBs [16–19]. However, so far all approaches still have physical problems in experimental realizations of the practically significant physical properties.

Recently we have proposed a photon echo QM in the optimal resonant cavity with CRIB technique for rephasing atomic coherence and demonstrated its effective integration into the quantum computer scheme [20]. The optical cavity approach provides a perfect time reversal retrieval of the multimode light fields for optically thin atomic system if an ideal CRIB procedure [6,21,22] can be successfully realized. Similarly the AFC protocol has been proposed for optical cavity [23]; meanwhile it cannot provide a time reversal dynamics. The recent experiment [24] has confirmed the possibility of photon echo QM with optically thin media. A perfect CRIB procedure in GEM technique can be implemented on the atomic ensembles provided that resonant line width is reduced to narrow homogeneous broadening for strong elimination of the atomic decoherence, but it decreases the effective optical depth and can lead to some experimental difficulties. For example, realization of CRIB procedure in optical cavity can disturb the cavity tuning and resonant interaction of the cavity mode with atomic ensemble. Thus it is highly desirable to find a simpler experimental solution to overcome the physical problems related to the rephasing of macroscopic coherence in IB atomic systems. In this paper we propose a simple scheme for a highly efficient multimode optical QM which resolves basic problems by using well-known experimental techniques. For this purpose we combine the specific advantages of the photon echo QM in an optical QED cavity with an off-resonant Raman type of atomic transition [25–28] in one scheme. Thus the proposed scheme almost ideally works with a natural IB line characterized by ultra-narrow homogeneous isochromatic components. Also the used optical cavity opens a convenient way for delicate rephasing of the atomic coherence excited in an IB system without significant excitation of the additional quantum noises and other undesirable negative effects with respect to the control laser fields and the predetermined atomic evolution. Below we describe a basic model and main physical properties of the proposed QM scheme. Then we summarize the critical physical requirements and outline the possible experimental realizations.

II. BASIC MODEL AND EQUATIONS

We analyze interaction of a three-level multiatomic system with a single mode optical cavity coupled with external signal field modes. It is assumed that all atoms ($j = 1,2,\ldots,N$) stay initially on the long-lived ground states $|1_a\rangle = \prod_{j=1}^{N} |1\rangle_j$ so the state of light and atoms is $|\Psi_{\rm in}\rangle = |\psi_f\rangle_{\rm in}|1_a\rangle$ before we launch any weak signal light field which can contain many temporally separated weak light pulses or even single photon fields. We analyze a sequence of single photon wave packets

*samoi@yandex.ru

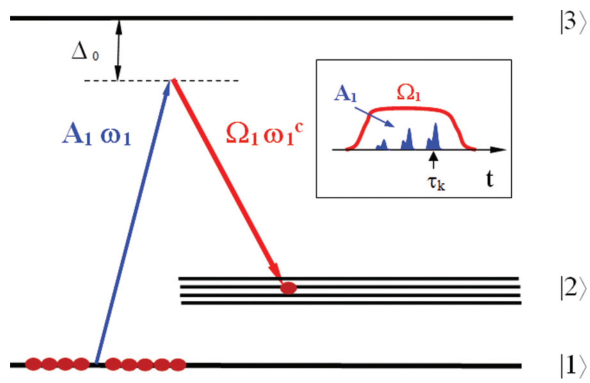

FIG. 1. (Color online) Energy level diagram and nonresonant Raman transition on the atomic transitions $|1\rangle \leftrightarrow |2\rangle$ due to the interaction with signal light pulse A_1 (with carrier frequency ω_1) and with control (writing) laser field; Ω_1 is a Rabi frequency on $|2\rangle \leftrightarrow |3\rangle$ transition and ω_1^c is a carrier frequency of the control field, Δ_0 is a sufficiently large resonant detuning from the optical transition. Inserted temporal diagram shows temporal shapes of the signal and control fields.

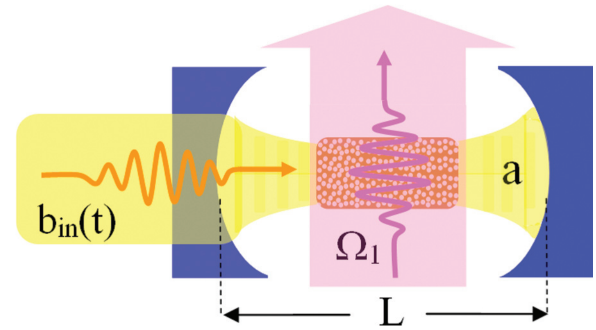

FIG. 2. (Color online) Spatial diagram of interaction between the atomic ensemble and optical cavity mode $\hat{a}$ in a presence of the control classical laser field Ω_1 propagating between the cavity mirrors, where the cavity mode is excited by input signal light field $\hat{b}_{\text{in}}(t)$.

prepared in the quantum state $|\psi_f\rangle_{\text{in}} = \prod_{k=1}^{M} \hat{\psi}_k^{\dagger}(t-\tau_k)\,|0\rangle$, $\hat{\psi}_k^{\dagger}(t-\tau_k) = \int_0^{\infty} d\omega_k f_k(\omega_k)\exp\{-i\omega_k(t-\tau_k)\}\hat{b}^{\dagger}(\omega_k)$, where f_k is a wave function in the frequency space normalized for pure single photon state $\int_0^{\infty} d\omega_k |f_k(\omega_k)|^2 = 1$, M is a number of temporal modes, and $\hat{b}^{\dagger}$ and $\hat{b}$ are the creation and annihilation operators of the frequency field modes $[\hat{b}(\omega'),\hat{b}^{\dagger}(\omega)] = \delta(\omega'-\omega)$, $|0\rangle = |0\rangle_m\,|0\rangle_f$ where $|0\rangle_m$ and $|0\rangle_f$ are the vacuum states of the cavity mode and of the free propagating field; kth photon mode arrives in the circuit at time moment τ_k, time delays between the nearest photons are assumed to be large enough $(\tau_k - \tau_{k-1}) \gg \delta t_k$, and $\delta t_k \approx \delta\omega_k^{-1}$ is a temporal duration of the kth field mode, with spectral width $\delta\omega_k \leqslant \delta\omega_f$, where $\delta\omega_f$ is an character spectral width.

We assume that central carrier frequency of the input signal fields coincides with the optical cavity mode frequency $\omega_{f,0} = \omega_o$, and the atomic ensemble is simultaneously exposed to an intense control laser field characterized by index $\nu = 1$ propagating along wave vector $\vec{K}_1$ with carrier frequency ω_1^c and Rabi frequency $\tilde{\Omega}_\nu(t,\vec{r}) = \Omega_\nu(t)\exp\{-i(\omega_\nu^c t - \vec{K}_\nu\vec{r})\}$ on a $|2\rangle \leftrightarrow |3\rangle$ atomic transition [where indexes $\nu = 1,\ldots,6$ are used for control laser fields in storage ($\nu = 1$), rephasing ($\nu = 2,3,4,5$), and retrieval ($\nu = 6$) stages of atomic and light evolution]. The excited cavity mode field A_1 and first control laser field Ω_1 provide off-resonant Raman excitation of atoms with a lambda scheme of quantum transition as depicted in Fig. 1.

A spatial diagram of the interaction presented in Fig. 2 shows an excitation of atoms by the cavity mode field $\hat{a}$ and control field Ω_1 propagating through the atomic medium without any reflection from the cavity mirrors. By following the cavity mode formalism for the coupling $\hat{V}_{m-f}$ of the cavity mode with external light field modes [29], we use a Tavis-Cummings Hamiltonian [30] for N three-level atoms $\hat{H}_a$ and its interaction with cavity mode $\hat{V}_{a-m}$ and with control field $\hat{V}_{a-c}$. Total atom-light Hamiltonian is

$$\hat{H} = \hat{H}_a + \hat{H}_m + \hat{H}_f + \hat{V}_{a-m} + \hat{V}_{a-c} + \hat{V}_{m-f}, \quad (1)$$

where $\hat{H}_a = \hbar\sum_{j=1}^{N}[\omega_{31}\hat{P}_{33}^j + (\omega_{21}+\delta^j)\hat{P}_{22}^j]$ is a Hamiltonian of three-level atoms, $\hat{P}_{nm}^j = |n\rangle_{jj}\langle m|$ is a projection operator of the jth atom, δ^j is a spectral detuning on $|1\rangle \leftrightarrow |2\rangle$ transition of the jth atom, and $\hat{H}_m = \hbar\omega_o\hat{a}^{\dagger}\hat{a}$ and $\hat{H}_f = \hbar\int \omega\hat{b}^{\dagger}(\omega)\hat{b}(\omega)d\omega$ are the Hamiltonians of the optical cavity mode and of free propagating modes coupled via the interaction term $\hat{V}_{m-f}$ and the interaction of atoms with optical cavity mode and with a classical control laser field are given by the Hamiltonians $\hat{V}_{a-m}$ and $\hat{V}_{a-c}$:

$$\hat{V}_{m-f} = -\hbar\int d\omega[\kappa(\omega)\hat{b}(\omega)\hat{a}^{\dagger} + \text{H.c.}],$$

$$\hat{V}_{a-m} = -\hbar\sum_{j=1}^{N}\{g_j\hat{a}\hat{P}_{31}^j + \text{H.c.}\}, \quad (2)$$

$$\hat{V}_{a-c} = -\hbar\sum_{j=1}^{N}\{\Omega_1(t)\exp\left[-i\left(\omega_1^c t - \vec{K}_1\vec{r}_j\right)\right]\hat{P}_{32}^j + \text{H.c.}\},$$

where $\hat{a}^{\dagger}$ and $\hat{a}$ are creation and annihilation operators of the cavity mode, $g_j = g_j^o\cos[\vec{k}\vec{r}_j]$, $g_j^o = \frac{\wp_{13}}{n}\sqrt{2\pi\omega/\hbar V}$ is the photon-atom coupling constant in optical cavity, $\wp_{13}$ is the dipole moment on the atomic transition $|1\rangle \leftrightarrow |3\rangle$, n is the refractive index of material, V is the quantization volume of the optical cavity [31,32], and $\vec{k}$ and $\vec{K}_1$ are the wave vectors of the standing cavity mode and of the first traveling control laser field.

By assuming a weak population of excited atomic states $|2\rangle$, $|3\rangle$ (i.e., $\langle\hat{P}_{22}^j\rangle \ll 1$ and $\langle\hat{P}_{33}^j\rangle \ll 1$) due to the interaction of multiatomic ensemble ($N \gg 1$) with weak single photon fields we will use the input-output field formalism [29] and derive the linearized system of Heisenberg equations for the field operators and for the atomic operators in the rotating frame representation $[\hat{b}(\omega) = \hat{b}_o(\omega)e^{-i\omega_s t}$, $\hat{a}(\omega) = \hat{a}_o(\omega)e^{-i\omega_s t}$, $\hat{P}_{13}^j = \hat{P}_{o,13}^j e^{-i\omega_s t}$, $\hat{P}_{12}^j = \hat{P}_{o,12}^j e^{-i\omega_{21}t}$ where ω_s is a carrier frequency of the input signal field $\hat{b}(t)]$ satisfying the condition of resonant Raman transition ($\omega_s - \omega_1^c \approx \omega_{21}$):

$$\frac{d}{dt}\hat{b}_o(\omega) = -i(\omega-\omega_s)\hat{b}_o(\omega) + i\kappa(\omega)\hat{a}_o, \quad (3)$$

$$\frac{d}{dt}\hat{a}_o = -i\left(\omega_o - \omega_s - i\frac{1}{2}\gamma_1\right)\hat{a}_o + i\sum_{j=1}^{N} g_j\hat{P}_{o,13}^j + \sqrt{\gamma_1}\hat{b}_{\text{in}}(t), \quad (4)$$

$$\frac{d}{dt}\hat{P}^j_{o,13} = -i\left(\Delta^j_{31} + \Delta_o\right)\hat{P}^j_{o,13} + ig^*_j\hat{a}_o, + i\Omega_1(t)\exp[i\vec{K}_1\vec{r}_j]\hat{P}^j_{o,12}, \quad (5)$$

$$\frac{d}{dt}\hat{P}^j_{o,12} = -i\delta^j\hat{P}^j_{o,12} + i\Omega^*_1(t)\exp[-i\vec{K}_1\vec{r}_j]\hat{P}^j_{o,13}, \quad (6)$$

where the input signal field containing M temporally separated photon wave packets is given by $\hat{b}_{\text{in}}(t) = \sum_{k=1}^{M}\hat{b}_{o,k}(t-\tau_k)$, where $\hat{b}_{o,k}(t-\tau_k) = \frac{1}{\sqrt{2\pi}}\int d\omega\hat{b}_o(\omega)\exp\{-i(\omega-\omega_s)(t-\tau_k)\}$, and $\gamma_1 = 2\pi\kappa^2(\omega_o)$ is a cavity loss rate, which can be also rewritten in the form $\gamma_1 = \omega_o/2Q$ [33], where Q is a quality factor of the optical cavity.

Let us assume that off-resonant Raman interaction of the cavity mode with atoms occurs for large enough spectral detuning between the carrier frequency of signal field ω_s and the frequency ω_{31} of optical atomic transition $|1\rangle \leftrightarrow |3\rangle$: $\Delta_o = \omega_{31} - \omega_s$, $|\Delta_o| \gg \delta\omega_f$. It is well known that in the case of sufficiently large spectral detuning $\Delta_o \gg \Delta^{(31)}_{\text{in}}$ (where $\Delta^{(31)}_{\text{in}}$ is IB of the transition $|1\rangle \leftrightarrow |3\rangle$) the excited optical atomic coherence evolves adiabatically following the cavity field and the long-lived atomic coherence in accordance with Eq. (5) and property of initial state $|\Psi_{\text{in}}\rangle$:

$$\hat{P}^j_{o,13}(t)|\Psi\rangle_{\text{in}} \cong \frac{1}{\Delta_o}\left\{g^*_j\hat{a}_o + \Omega_1(t)\exp[i\vec{K}_1\vec{r}_j]\hat{P}^j_{o,12}\right\}|\Psi_{\text{in}}\rangle. \quad (7)$$

Total IB of the Raman transition will be determined only by inhomogeneous broadening $G(\delta/\delta_{\text{in}})$ on the atomic transition $|1\rangle \leftrightarrow |2\rangle$ (δ_{in} is an IB line width of the atomic transition). It is highly preferable for many aspects of quantum storage if $|1\rangle \leftrightarrow |2\rangle$ will be a highly forbidden atomic transition (see below). It is worth noting the adiabatic evolution (7) requires a large spectral detuning $|\Delta_o| > |\Omega_1|$, and we can use $|\Omega_1/\Delta_o| \approx 0.1$ in order to provide highly efficient and a fast switching rate of the control field (principally we can use even larger spectral detuning $|\Omega_1/\Delta_o| < 0.1$ by appropriate optimization of the atomic and light parameters). Factor $|\Omega_1/\Delta_o| \ll 1$ decreases an effective optical depth of the atomic system; however, this problem is resolved here due to considerable enhancement of light atoms' interaction in the optical cavity.

Putting Eq. (7) in Eqs. (4) and (6) and assuming $\omega_s = \tilde{\omega}_o$, $\delta^j = \Delta^j_{21} - \Omega_1/\Delta_o$, $\tilde{g}_j = g_j\exp[i\vec{K}_1\vec{r}_j]$ and $\tilde{\omega}_o = \omega_o - N\overline{g}^2/\Delta_o$ (where $\overline{g} = \sqrt{\sum_{j=1}^{N}|\tilde{g}_j|^2/N}$) we get two light atoms equations:

$$\frac{d}{dt}\hat{a}_o = -\frac{1}{2}\gamma_1\hat{a}_o + i\frac{\Omega_1(t)}{\Delta_o}\sum_{j=1}^{N}\tilde{g}_j\hat{P}^j_{o,12} + \sqrt{\gamma_1}\hat{b}_{\text{in}}(t), \quad (8)$$

$$\frac{d}{dt}\hat{P}^j_{o,12} = -i\left(\delta^j - i\frac{1}{T_2}\right)\hat{P}^j_{o,12} + i\frac{\Omega^*_1(t)}{\Delta_o}\tilde{g}^*_j\hat{a}_o + \hat{F}^j_{12}, \quad (9)$$

where for generalization we have also introduced a small decay constant $1/T_2$ of the atomic coherence and δ-correlated Langevin noise operators $\hat{F}^j_{12}$ determined by the interaction of atoms with surrounding host atoms and with bath electromagnetic fields. We will be interested in a solution of Eqs. (8) and (9) in the limit of the negligibly weak influence of the atomic decoherence and corresponding Langevin noise. A coupled system of Eqs. (3), (8), and (9) describe the interaction of optical cavity mode and resonant three-level atomic system under the action of input light signal $\hat{b}_{\text{in}}(t)$. The equations coincide formally with the light atom equations for the photon echo QM on two-level atoms in optical cavity [20] if we replace the photon-atom coupling constant g_j by the controlled effective coupling constant $i\frac{\Omega^*_1(t)}{\Delta_o}\tilde{g}_j$.

III. QUANTUM STORAGE

By assuming the control field is switched on to the constant magnitude Ω_1 before the signal pulse arrives in the optical cavity at $t = 0$, we realize a storage of the input signal on the atomic coherences $\hat{P}^j_{o,12}$ and $\hat{P}^j_{o,13}$ after complete arrival of all the M signal light pulses $\hat{a}_o(t > \tau_M + \delta t_M)|\Psi_{\text{in}}\rangle = 0$. Further adiabatic switching of the control laser field for $t > \tau_M + \delta t_M + \tilde{\tau}$ leads to

$$\hat{P}^j_{o,12}(t) = i\sqrt{2\pi}\frac{\Omega^*_1}{\Delta_o}\tilde{g}^*_j\hat{a}_o(\delta^j)e^{-i(\delta^j - i/T_2)t}, \quad (10)$$

$$\hat{a}_o(\nu) = \frac{\sqrt{\gamma_1}\hat{b}_{\text{in}}(\nu)}{\frac{1}{2}\gamma_1 - i\nu - i\frac{1}{2}\Gamma_r\delta_{\text{in}}\int\frac{d\delta G(\delta/\delta_{\text{in}})}{\delta - \nu - i/T_2}}, \quad (11)$$

where $\hat{a}_o(\nu) = \frac{1}{\sqrt{2\pi}}\int dt e^{i\nu t}\hat{a}_o(t)$, $\hat{b}_{\text{in}}(\nu) = \frac{1}{\sqrt{2\pi}}\int dt e^{i\nu t}\hat{b}_{\text{in}}(t) = \sum_{k=1}^{M}e^{i\nu\tau_k}\hat{b}_o(\nu)$, $\Gamma_r = 2N|\frac{\Omega_1}{\Delta_o}\overline{g}|^2/\delta_{\text{in}}$, and $\hat{P}^j_{o,13}(t)|\Psi_{\text{in}}\rangle = 0$. The excited atomic coherence in Eq. (10) contains only the term which is essential for quantum efficiency storage and fidelity of the studied process. We have ignored the Langevin forces in the excited atomic coherence since it vanishes in the limit of negligible weak atomic decoherence, while the factor e^{-t/T_2} in Eq. (10) is kept for evaluation of the relative impact of the decoherent processes on the excited atomic coherence in the studied limit.

By using for simplicity the Lorentzian shape of IB $G_g(\delta/\delta_{\text{in}}) = \frac{\delta_{\text{in}}}{\pi(\delta^2 + \delta^2_{\text{in}})}$ in Eqs. (10) and (11) we calculate a storage efficiency of the signal field $Q_{ST}(t) = \bar{P}_{22}(t)/\bar{n}_1$ where $\bar{P}_{22}(t) = \sum_{j=1}^{N}\langle\hat{P}^j_{o,21}(t)\hat{P}^j_{o,12}(t)\rangle$ is an excited number of atoms after the interaction with M signal fields for $t > \tau_M + \delta t_M$ (where $\delta t_M \approx \delta\omega_f^{-1}$). The total number of photons in the input signal field is $\bar{n} = \sum_{k=1}^{M}\bar{n}_k$, where $\bar{n}_k = \int_{-\infty}^{\infty}dt\langle\hat{b}^{\dagger}_{o,k}(t)\hat{b}_{o,k}(t)\rangle$ is the input number of photon in kth temporal mode, and $\langle\cdots\rangle$ is a quantum averaging over the initial state $|\Psi_{\text{in}}\rangle$.

Performing the algebraic calculations of $\bar{P}_{22}(t)$, we find the quantum efficiency of storage $Q_{ST} = (1/\bar{n}_1)\sum_{k=1}^{n}Q_{ST,k}\bar{n}_k$ where the storage efficiency of kth mode is

$$Q_{ST,k} = \int_{-\infty}^{\infty}d\nu Z_r(\nu,\delta_{\text{in}},T_2,\gamma_1,\Gamma_r)\frac{\langle\hat{n}_k(\nu)\rangle}{\bar{n}_k}, \quad (12)$$

where *spectral storage* (SS) function $Z_r(\nu,\delta_{\text{in}},T_2,\gamma_1,\Gamma_r) = |S_r(\nu,\delta_{\text{in}},T_2,\gamma_1,\Gamma_r)|^2$ and S function $S_r(\nu,\ldots)$ is

$$S_r(\nu,\delta_{\text{in}},T_2,\gamma_1,\Gamma_r) = \sqrt{\frac{\delta^2_{\text{in}}}{(\delta^2_{\text{in}} + \nu^2)}}\frac{2\sqrt{\gamma_1\Gamma_r}}{\left[\gamma_1 + \Gamma_r\frac{\delta_{\text{in}}}{(\delta_{\text{in}} + 1/T_2 - i\nu)} - 2i\nu\right]} \quad (13)$$

and characterizes the quantum storage $Q_{ST,k}$ for the νth spectral component of the kth light temporal mode. It is worth noting that SS function $Z_r(\nu,\ldots)$ differs only by parameter Γ_r from the similar SS function in the photon echo QM on two-level atoms studied in Ref. [20], where Γ_r characterizes a photon absorption rate on the off-resonant Raman transition. We note that Eq. (12) demonstrates a quite typical property of the photon or spin echo-based storage in free propagation geometry or in the optical cavity schemes. Here each spectral component of the input light field is transferred on the resonant spectral component of the excited atomic coherence where the quantum efficiency for each spectral component is determined by the SS function $Z_r(\nu,\delta_{\text{in}},T_2,\gamma_1,\Gamma_r)$. By assuming $1/T_2 \ll \delta_{\text{in}}$ from Eqs. (12) and (13) we get the following two conditions for realization of efficient quantum storage: (1) $\Gamma_r = \gamma_1$ and (2) $\delta_{\text{in}} = \gamma_1/2$.

The first one is an well-known impedance matching condition in laser physics [34,35] modified by the Raman atomic transition. By taking into account $\gamma_1 \approx Tc/(2L)$ [where $T = 1 - R$ and R are the transmission and reflection coefficients (for the left mirror in Fig. 2), c is a speed of light, L is a longitudinal length of the optical cavity], we get for the transmission coefficient $T = 2\chi\alpha_r L$, where the absorption coefficient on the Raman transition $\alpha_r = |\frac{\Omega_1}{\Delta_o}|^2 \frac{\Delta_{\text{in}}^{(13)}}{\delta_{\text{in}}}\alpha_{13}$ and $\alpha_{13} = 4\pi n_o \frac{|\wp_{13}|^2\omega_{31}}{c\hbar\Delta_{\text{in}}^{(13)}}$ is an absorption coefficient on the optical transition, $n_o = \frac{N}{V_a}$ atomic density, V_a volume of atomic medium, $\chi = V_a/(LS)$ is a filling factor of the cavity by the atomic system, and S is an averaged cross section of the cavity mode.

Thus instead of the strict demand on the resonant optical depth $\alpha_r L \gg 1$ in the case of a free space QM [6], we have a quite weaker demand even for the Raman scheme of atomic transition. We rewrite the condition for the absorption coefficient $\alpha_r = T/(2\chi L)$, which can be easily realized in experiments with optical QED cavities. To give an example, let us assume $\gamma_1 = 10^8\ \text{s}^{-1}$ and $L = 0{,}1$ cm (or 1 cm); we get $T \cong 0.7\times 10^{-3}$ (or $T \cong 0.7\times 10^{-2}$). By assuming also $\chi = 0.5$ and $|\frac{\Omega_1}{\Delta_o}|^2 = 0.01$ we get the matching condition for the optical absorption coefficient $\alpha_{13} = 0.7\,\delta_{\text{in}}/\Delta_{\text{in}}^{(13)}$ independent of L. Usually $\delta_{\text{in}}/\Delta_{\text{in}}^{(13)}$ lays in the range 0.1–0.01 for rare-earth ions in the inorganic crystals [4,36] where $\Delta_{\text{in}}^{(13)} \approx 10^9$–$10^{10}\ \text{s}^{-1}$. It particular for the optical transition ${}^3H_4{-}{}^1D_2$ in $Pr^{3+} : Y_2SiO_5$ we can find the following parameters: $\lambda = 605.977$ nm, $\wp_{13} = 1.59\times 10^{-32}$ cm, $T_2 = 152\ \mu$s, coupling constant $g \cong 1.1\times 10^6\ \text{s}^{-1}$ for quantization volume $V = 10^{-8}\ \text{m}^{-3}$ and refractive index of material $n = 1.8$ [37]. If we take into account $\Gamma_r = \gamma_1 = 2\delta_{\text{in}} = 10^8\ \text{s}^{-1}$ and $\frac{\Omega_1^2}{\Delta_o^2} \approx 10^{-2}$ it leads to the following optimal number of atoms in this cavity volume: $N = \frac{\gamma_1\delta_{\text{in}}\Delta_o^2}{2\Omega_1^2 g^2} \approx \frac{1}{4}\times 10^6$. The quantity corresponds to the quite low concentration of ions Pr^{3+} $n_o = \frac{1}{4}\times 10^{14}\ \text{cm}^{-3}$ or using small filling factor $\chi \approx 10^{-4} - 10^{-5}$ (or $\frac{\Omega_1^2}{\Delta_o^2} \ll 10^{-2}$) for typical ion concentration $n_o = 4.7\times 10^{18}\ \text{cm}^{-3}$ in this crystal [36].

The performed estimation indicates a relatively easy experimental realization of the modified matching condition in the optical cavities. In other words, the matching condition provides a possibility of using the atomic ensembles with a quite small optical absorption coefficients $\alpha_{13} < 0.1$ (for each isochromatic group of atoms within IB line). This also means a possibility of lower density of the resonant atoms and weaker interatomic dipole-dipole interactions, respectively, which also promises a larger lifetime of the atomic coherence T_2. We also note that we can vary IB line width δ_{in} in external constant electrical or magnetic fields without using a CRIB procedure for perfect retrieval.

It is worth noting off-resonant Raman interaction facilitates an experimental realization of the impedance matching condition due to the possible tuning of Rabi frequency Ω_1 and spectral detuning Δ_o: $|\frac{\Omega_1}{\Delta_o}| = \sqrt{\frac{\delta_{\text{in}}\gamma_1}{2N|\bar{g}|^2}}$, which is important for the atomic media with arbitrary number N of effective three-level atoms.

Another well-known important advantage of the Raman scheme is a direct mapping of the input light fields on the long-lived atomic transition $|1\rangle \leftrightarrow |2\rangle$ so the transition can be completely forbidden for realization of spontaneous coherent atomic irradiation on this transition, and this atomic transition will suppress many relaxation processes providing a large T_2 for long-lived storage of the input signal fields.

The second condition called the *optimal spectral matching condition* [20] demonstrates an optimal coupling of the spectral shapes related to the atomic IB and optical cavity window transparency, which provides an effective quantum storage for broadened spectral range of input signal fields where the SS function $Z_r(\nu,\ldots) \cong 1$.

The excited atomic systems is characterized by completely dephased coherence (10) on the transition $|1\rangle \leftrightarrow |2\rangle$, and the light field retrieval requires a perfect rephasing of the atomic coherence for subsequent irradiation of the echo field. Let us now consider the retrieval stage.

IV. RETRIEVAL STAGE

A. Rephasing of atomic coherence

Retrieval still remains the most critical stage in the photon echo QMs. Here we propose an efficient solution of this problem by using the specific advantages of Raman-based techniques for the atomic coherent control in optical cavity. Moreover we implement the retrieval for the atomic system with natural IB of atomic transition $|1\rangle \leftrightarrow |2\rangle$ without any dynamical or static manipulations of the atomic spectral detunings used in CRIB [4,6,7,22] and in AFC [9] techniques for rephasing of excited IB atomic coherence. Despite the recently proposed photon echo QM techniques also based on the natural IB [16–19], the efficient experimental realization of these schemes still requires additional improvements which would eliminate the specific physical shortcomings caused by extra quantum noises and limited quantum efficiency.

Our scheme makes use of the additional experimental tools for realization of perfect manipulation of the atomic coherence providing highly efficient rephasing of the long-lived coherence $\hat{P}_{o,12}(t)$ (10) excited on the natural IB transition. To start the coherence rephasing at time $t = t_o$ we launch two intensive laser fields ($\nu = 2{,}3$) exciting off-resonant Raman atomic transition $|1\rangle \leftrightarrow |2\rangle$ in the following way. As is shown in the spatial scheme in Fig. 3, the laser pulses simultaneously propagate between the two mirrors of an optical cavity. It is taken into account the pulses can propagate in an arbitrary angle to each other (they could be even in opposite directions).

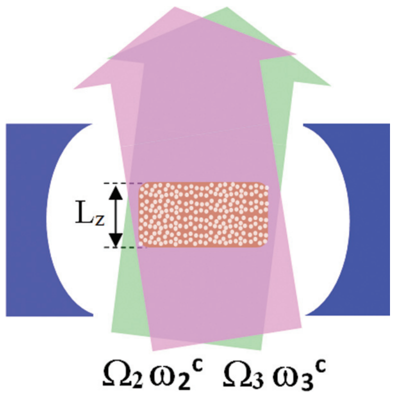

FIG. 3. (Color online) Spatial scheme of the atomic excitation by two control fields Ω_2 and Ω_3 satisfying the Raman resonance with atomic transition $|1\rangle \leftrightarrow |2\rangle$: $\omega_2^c - \omega_3^c \approx \omega_{21}$. The fields can propagate in arbitrary directions between the cavity mirrors.

This can be realized for the cases discussed in the previous section, where, for example, the distance between two mirrors of the optical cavity can range from 1 mm to 1 cm. We also assume the input laser pulses parameters provide a perfect quantum transition $|1\rangle \leftrightarrow |2\rangle$ characterized by the pulse area equal to π. Also we can implement the excited transient optical coherences $\hat{P}_{o,13}(t)$ and $\hat{P}_{o,23}(t)$ are not coupled with any cavity modes since the carrier frequencies of the laser pulses ω_2^c and ω_3^c can be shifted from the resonant frequencies of the cavity modes as depicted in Fig. 4.

In comparison with the properties of usual photon echo QM schemes, we show the control intensive light fields will propagate through a medium in our scheme without significant backward influence of the atomic medium; i.e., the atomic system can be characterized by negligibly small optical depth for the control laser fields. In order to clarify the noted key scheme advantages we examine the light atoms dynamics for the case of short control light pulses, and then we characterize the optimal atomic parameters. Similarly to the storage stage we assume a sufficiently large optical detuning $\Delta_{0,2} = \omega_{31} - \omega_2^c$ (see Fig. 4 where $|\Delta_{0,2}| > \Delta_0$) that determines adiabatic relations for the optical coherences:

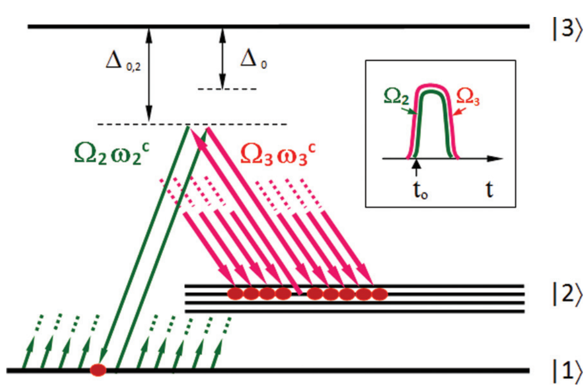

FIG. 4. (Color online) Two control lasers Ω_2 and Ω_3 invert atomic state on the transition $|1\rangle \leftrightarrow |2\rangle$ via off-resonant Raman transition characterized by another spectral detuning on the optical transition ($\Delta_{0,2} \neq \Delta_0$ so the laser field frequencies do not coincide with the optical cavity frequency: $\omega_2^c \neq \omega_o$ $\omega_3^c \neq \omega_o$); the arrows demonstrate a perfect π-pulse area of the excitation for the atoms. The insert figure shows temporal diagram for two control rephasing laser fields ($\nu = 2,3$) with coincided temporal shapes.

$$\hat{P}^j_{o,13} \cong \frac{1}{\Delta_{0,2}}\{\Omega_2(t)e^{ik_2r_j}(\hat{P}^j_{o,11} - \hat{P}^j_{o,33}) + \Omega_3(t)e^{ik_3r_j}\hat{P}^j_{o,12}\},$$
$$\hat{P}^j_{o,23} \cong \frac{1}{\Delta_{0,2}}\{\Omega_3(t)e^{ik_3r_j}(\hat{P}^j_{o,22} - \hat{P}^j_{o,33}) + \Omega_2(t)e^{ik_2r_j}\hat{P}^j_{o,21}\}, \tag{14}$$

and leads to the dynamic equations for atomic evolution determined by the well-known effective Hamiltonian $\hat{H}_{\text{eff},1}(t) = \sum_{j=1}^N \hat{H}^j_{\text{eff},1}(t)$ where $\hat{H}^j_{\text{eff},1}(t) = \hbar\delta^j(t)\hat{P}^j_{22} + \hat{V}_j(t)$ and the light atom interaction term:

$$\hat{V}_j(t) = -\hbar\left\{\frac{\Omega_{2,j}(t)\Omega^*_{3,j}(t)}{\Delta_{0,2}}\hat{P}^j_{0,12}e^{-i(k_2-k_3)r_j} + \text{H.c.}\right\}, \tag{15}$$

where $\delta^j(t) = \delta^j - \frac{|\Omega_{2,j}(t)|^2 - |\Omega_{3,j}(t)|^2}{\Delta_{0,2}}$ $\Omega_{2,j}(t) = \wp_{13}E_2(t,r_j)/\hbar$ is an atomic detuning, $\Omega_{3,j}(t) = \wp_{23}E_e(t,r_j)/\hbar$ are Rabi frequencies for the jth atom of the second and third control laser pulse on $|1\rangle \leftrightarrow |3\rangle$ and $|2\rangle \leftrightarrow |3\rangle$ atomic transitions, and $\wp_{13}$ and $\wp_{23}$ are the appropriate dipole moments of the atomic transitions.

The effective Hamiltonian $\hat{H}^j_{\text{eff},1}$ determines the following atomic equations:

$$\frac{d}{dt}\hat{P}^j_{o,12} = -i\left(\delta^j - \frac{|\Omega_2(t)|^2 - |\Omega_3(t)|^2}{\Delta_{0,2}}\right)\hat{P}^j_{o,12} + i\frac{\Omega_2(t)\Omega_3^*(t)}{\Delta_{0,2}}e^{i(k_2-k_3)r_j}\hat{W}^j, \tag{16}$$

$$\frac{d}{dt}\hat{W}^j = -2i\left(\frac{\Omega_2(t)\Omega_3^*(t)}{\Delta_{0,2}}\hat{P}^j_{o,21}e^{i(k_2-k_3)r_j} - \text{H.c.}\right), \tag{17}$$

where $\hat{W}^j = \hat{P}^j_{o,11} - \hat{P}^j_{o,22}$, $\frac{d}{dt}\hat{P}^j_{o,11} = -\frac{d}{dt}\hat{P}^j_{o,22}$, equations for $\hat{P}^j_{o,nm}$ $(n,m = 1,2,3; n \neq m)$ are the Hermitian conjugated equations for $\hat{P}^j_{o,mn}$.

By assuming a negligibly small angle between the propagation directions we write the equations for slowly varied amplitudes of the control light fields $E_2(t,z)$ and $E_3(t,z)$:

$$\left(\frac{\partial}{\partial z} + \frac{1}{c}\frac{\partial}{\partial t}\right)E_2(t,z) = i\beta_1 e^{-ik_2z}\langle P_{0,13}(t,z)\rangle, \tag{18}$$
$$\left(\frac{\partial}{\partial z} + \frac{1}{c}\frac{\partial}{\partial t}\right)E_3(t,z) = i\beta_2 e^{-ik_3z}\langle P_{0,23}(t,z)\rangle, \tag{19}$$

where $\beta_p = \frac{2\pi}{c}\omega_{3p}n_o\wp_{p3}$, $(p = 1,2)$, $\langle P_{0,13}(t,z)\rangle$ and $\langle P_{0,23}(t,z)\rangle$ are the macroscopically averaged atomic coherences, the z axis is orthogonal to the longitudinal axis of the cavity (see Fig. 3).

Let us analyze the propagation effects of the fields $E_2(t,z)$ and $E_3(t,z)$ by assuming a short input temporal durations of the laser pulses in order to neglect by any influence of IB on the transition $|1\rangle \leftrightarrow |2\rangle$ (i.e., $\delta_{\text{in}} \cdot \delta t_{2,3} \ll 1$). Also we assume initial Rabi frequencies are equaled to each others $[\Omega_2(t) = \Omega_2^*(t) = \Omega_3(t) = \Omega_3^*(t)]$. It leads to the following solution of Eqs. (16) and (17):

$$\hat{P}^j_{o,12}(t) = \cos^2[\Theta(t)/2]\hat{P}^j_{o,12}(\tau_o) + \sin^2[\Theta(t)/2]\hat{P}^j_{o,21}(\tau_o) \times e^{2i(k_2-k_3)r_j} + i\tfrac{1}{2}e^{i(k_2-k_3)r_j}\sin[\Theta(t)/2]\hat{W}^j(\tau_o), \tag{20}$$

$$\hat{W}^j(t) = \cos\Theta(t)\hat{W}^j(\tau_o) + \sin\Theta(t)\{\hat{P}^j_{o,21}(\tau_o)e^{i(k_2-k_3)r_j} - \hat{P}^j_{o,12}(\tau_o)e^{-i(k_2-k_3)r_j}\}, \quad (21)$$

where $\Theta(t) = 2\int_{t_o}^{t} dt \frac{\Omega_2(t)\Omega_3(t)}{\Delta_{0,2}}$, $\hat{P}^j_{o,12}(\tau_o)$ is determined by initially excited atomic coherence (10), $\{\hat{P}^j_{o,21}(\tau_o) = [\hat{P}^j_{o,21}(\tau_o)]^\dagger\}$, and $\hat{P}^j_{o,22}(\tau_o)$ is determined appropriately.

By taking into account the solutions (20) and (21) in Eqs. (18) and (19) and negligibly weak initial population of excited levels $[\langle\hat{P}_{o,22}(\tau_o)\rangle \ll 1,\ \langle\hat{P}_{o,33}(\tau_o)\rangle = 0]$ due to excitation by the input signal light we write the field equations in the moving system of coordinate ($Z = z$, $\tau = t - z/c$) in terms of its Rabi frequencies:

$$\frac{\partial}{\partial Z}\Omega_2 = -\frac{1}{2}\alpha_{r,13}\left\{\frac{\Omega_3}{2}\sin\Theta - i\Omega_2\cos^2[\Theta/2]\right\}, \quad (22)$$

$$\frac{\partial}{\partial Z}\Omega_3 = \frac{1}{2}\alpha_{r,23}\left\{\frac{\Omega_2}{2}\sin\Theta + i\Omega_3\sin^2[\Theta/2]\right\}. \quad (23)$$

The nonlinear system of the control field equations (22) and (23) show that possible influence of absorption(amplification) and dispersion effects are determined by the coupling constants $\alpha_{r,p3} = \frac{\Delta_{\text{in}}^{p3}}{\Delta_{0,2}}\alpha_{p3}$ (where $p = 1,2$) and spatial length $L_z \cong S^{1/2}$ of the medium in the cross section of an optical cavity. For evaluation we assume equal IB widths $\Delta_{\text{in}}^{(23)} = \Delta_{\text{in}}^{(13)}$ and absorption coefficients $\alpha_{23} = \alpha_{13}$ in Eqs. (22) and (23), which leads to the equation for effective pulse area $\Theta(\tau,Z)$:

$$\frac{\partial^2}{\partial Z\partial\tau}\Theta = \frac{1}{2}\alpha_{r,13}\left\{\frac{\Omega_2^2 - \Omega_3^2}{\Delta_{0,2}}\sin\Theta + i\frac{\partial}{\partial\tau}\Theta\right\}. \quad (24)$$

By taking into account the equal control field magnitudes ($\Omega_2^2 - \Omega_3^2 = 0$) we find the main influence of light atom interaction leads to the phase rotation $\Theta(\tau,Z) \cong \Theta(\tau,0)\exp\{i\frac{1}{2}\alpha_{r,13}Z\}$ that can change the phase-matching condition in the medium only in the case of sufficiently large effective optical depth $\frac{1}{2}\alpha_{r,13}L_z$. Similar evolution will occur for other parameters of the control fields, such as $\Omega_2(\tau,Z)$, $\Omega_3(\tau,Z)$ and $\Omega_2^2(\tau,Z) - \Omega_3^2(\tau,Z)$.

We can estimate the evolution of control light field parameters by taking into account the optimal absorption coefficient and spatial properties of the atomic medium discussed in the previous section. In accordance with the discussion, the first matching condition is determined by the longitudinal length of the cavity and absorption coefficient α_{13} so we can use a small cross section of the cavity with $L_z \ll L$ where minimal spatial length L_z can be limited by the a few wavelengths of the cavity mode. For experimental convenience we can use larger spatial length $L_z \approx L = 1$ mm. Even for this case we have $\frac{1}{2}\alpha_{r,13}L_z \ll 1$ since $\frac{\Delta_{\text{in}}^{p3}}{\Delta_{0,2}} \ll 1$ and $\alpha_{r,13}L_z \ll 1$ so with high accuracy the effective pulse area Θ will not be changed in the atomic medium. Moreover one can realize $\Theta(Z) = \Theta(0)$ with *a priori* given arbitrary accuracy since the negligibly small effective optical depth of the atomic system along the z direction can be realized by a sufficiently high transverse confinement of the optical cavity mode field and appropriate transverse medium size. It is clear that in this case of effectively small optical depth we obtain the same result for different values of the absorption coefficients $\alpha_{r,13}$ and $\alpha_{r,23}$ and its IB widths. Thus we can neglect by any backward action of the atomic medium to the control light fields which provides a uniform evolution of the atomic coherences determined by the input parameters of control laser pulses with fixed equal real Rabi frequencies $\Omega_2(t) = \Omega_3(t)$ with an effective pulse area Θ. Quantum dynamics of any jth atomic operator in the laboratory system of coordinates will be determined as follows: $\hat{P}^j_{0,nm}(t = \delta t_2 + t_o) = \hat{U}^\dagger_j(\Theta)\hat{P}^j_{0,nm}(t_o)\hat{U}_j(\Theta)$ where $\hat{U}_j(\Theta) = \exp\{-i\frac{\Theta}{2}[\hat{P}^j_{0,12}e^{-i(k_2-k_3)r_j} + \text{H.c.}]\}$, δt_2 is a temporal duration of the control laser pulses (the temporal durations of the control laser pulses are assumed to be a negligibly short).

Here we assume $\Theta = \pi$ that leads to the perfect inversion of atomic states on the transition $|1\rangle \leftrightarrow |2\rangle$. We note it is difficult to realize such perfect inversion of all two-level atomic ensemble via applying an intensive resonant light pulse in a single mode optical cavity due to many reasons. For example, such a π pulse immediately leads to the effect of Dicke superradiance [38] and enhances strong interatomic interactions. In the free propagating scheme it leads to strong nonlinear light propagation effects of self-induced transparency in the echo irradiation [39–41], which can be accompanied by strong dispersion effects [18] and even by soliton pulse formation [42,43]. Here it is also worth noting the atoms in the studied scheme are excited to the forbidden transition $|1\rangle \leftrightarrow |2\rangle$, which is also out of any resonance with optical cavity modes. Thus our scheme provides a robust perfect inversion of atomic states without essential interparticle interactions and interaction with the optical cavity modes.

Subsequent evolution of the atomic coherence will be determined by the Hamiltonian $\hbar\delta^j\hat{P}^j_{22}$ containing only different spectral atomic detuning $\hat{P}^j_{0,12}(T_o + \delta t_2 + t_o) = \hat{T}^\dagger_j(T_o)\hat{P}^j_{0,12}(\delta t_2 + t_o)\hat{T}_j(T_o)$. A complete procedure of the atomic rephasing contains action of two pairs of the control laser pulses separated by time delay $T_o > t_o - \tau_k$, where $t_o - \tau_k$ is a dephasing time for kth temporal mode (see Fig. 5), where each pair of laser pairs provides effective pulse area π of the atomic excitation that leads to the following behavior of the long-lived atomic coherence:

$$\begin{aligned}\hat{P}^j_{0,12}&(\delta t_4 + T_o + \delta t_2 + t_o)\\ &= \hat{U}^\dagger_j(\pi)\hat{T}^\dagger_j[T_o]\hat{U}^\dagger_j(\pi)\hat{P}^j_{0,12}(t_o)\hat{U}_j(\pi)\hat{T}_j[T_o]\hat{U}_j(\pi)\\ &= -e^{i\delta^j T_o}\hat{P}^j_{0,12}(t_o). \end{aligned} \quad (25)$$

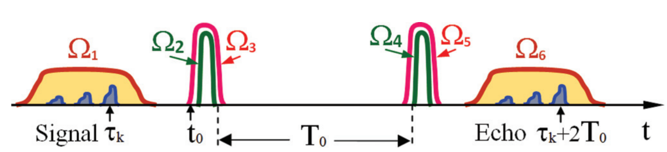

FIG. 5. (Color online) Temporal scheme. The input signal (three blue (dark) pulses) enters the medium in the presence of first writing laser field Ω_1; two pairs of the control laser pulses Ω_2,Ω_3 and Ω_4,Ω_5 with effective pulse areas π are applied for rephasing the excited atomic coherence; reading laser pulse Ω_6 initiates echo field emission characterized by the same temporal shape and order as it is for the input signal field.

Thus the recovered atomic coherence $\hat{P}^j_{0,12}(t)$ at time moment $t = \delta t_4 + T_o + \delta t_2 + t_o$ acquires an additional phase $\delta^j T_o$ of the opposite sign with respect to the atomic phase excited after the signal field absorption. The rephasing process is highly immune to main negative physical processes usually limiting the quantum efficiency caused by light field propagation in the optical dense media and excitation of atoms on the excited allowed quantum states. Basically the accuracy of the rephasing is limited only by the accuracy of tuning of effective pulse area related to the control laser fields. In order to increase the accuracy of atomic inversion on the transition $|1\rangle \leftrightarrow |2\rangle$ we can also apply a so-called counterintuitive pulse sequence in the well-known STIRAP scheme [31], which could provide a robust perfect Raman transfer of atoms for relatively arbitrary intensities of the laser pulses.

B. Echo field emission

In order to retrieve the stored quantum state we launch an additional sixth reading laser pulse at time $t > t_o + T_o$ (see Fig. 5) when the initial state of atomic coherence is defined by Eqs. (10) and (25). The reading pulse switches on the coherent light atoms interaction due to the evolving rephasing of atomic coherence on the transition $|1\rangle \leftrightarrow |2\rangle$ when the cavity mode evolves from the vacuum state. Let us assume the reading laser pulse is characterized by Rabi frequency Ω_6, and its carrier frequency coincides with the frequency of first (writing) control laser field $[\Omega_6(\tilde{t}) = \Omega_1(\tilde{t}), \omega^c_6 = \omega^c_1]$. In this case after complete switching on, we obtain the same equations for the free propagating modes (3) and a similar system of equations for the atomic coherence $\hat{P}^j_{0,12}$ and cavity mode Eqs. (8) and (9) but without an external light field source:

$$\frac{d}{dt}\hat{a}_o = -\frac{1}{2}\gamma_1\hat{a}_o + i\frac{\Omega_6}{\Delta_o}\sum_{j=1}^{N}\tilde{g}_j\hat{P}^j_{o,12}, \tag{26}$$

$$\frac{d}{dt}\hat{P}^j_{o,12} = -i\left(\delta^j - i\frac{1}{T_2}\right)\hat{P}^j_{o,12} + i\frac{\Omega^*_6}{\Delta_o}\tilde{g}^*_j\hat{a}_o. \tag{27}$$

By using the Laplace transformations in Eqs. (26) and (27) we find the solution for the cavity mode field

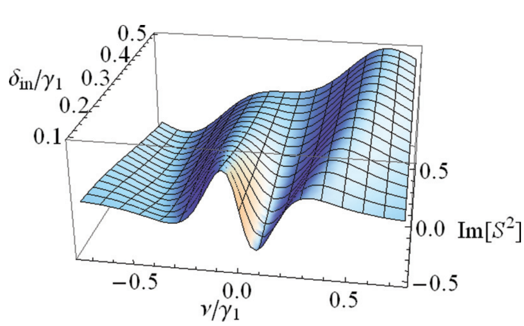

FIG. 6. (Color online) Imaginary part of the square of S function (Im[S^2]) for small inhomogeneous broadening $0.1 < \delta_{\rm in}/\gamma_1 < 0.5$ where almost zero phase modulation occurs within spectral range $-0.25 < \nu/\gamma_1 < 0.25$ if inhomogeneous broadening width $\delta_{\rm in} \approx 0.5\gamma_1$.

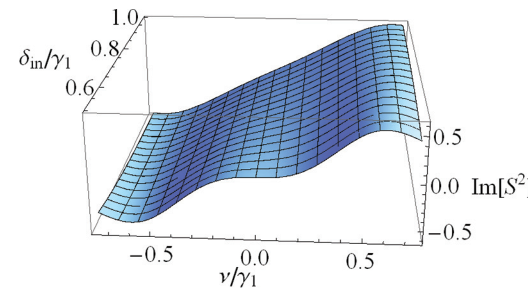

FIG. 7. (Color online) Imaginary part of the square of S function for larger inhomogeneous broadening $\delta_{\rm in}$; we see almost linear phase modulation within spectral range $-0.25 < \nu/\gamma_1 < 0.25$ for large $\delta_{\rm in}$: $\delta_{\rm in} \gg 0.5\gamma_1$. The linear phase modulation leads only to additional time shift of each echo pulse irradiation without its temporal rephasing.

$\hat{a}_o(t) = \sum_{k=1}^{M}\exp\{-(t-\tau_k)/T_2\}\hat{a}_{e,k}(t)$ where

$$\hat{a}_{e,k}(t) = \frac{1}{\sqrt{2\pi\gamma_1}}\int_{-\infty}^{\infty}d\nu\hat{b}_o(\nu)[S_r(\nu,\delta_{\rm in},T_2,\gamma_1,\Gamma_r)]^2 \times \exp\{-i\nu(t-2T_0-\tau_k)\}. \tag{28}$$

Then using (28) in (3) we find for the echo field $\hat{b}_o(t) = \sqrt{\gamma_1}e^{-2T_o/T_2}\sum_{k=1}^{M}\hat{a}_{e,k}(t)$. Thus we see if S function $S_r(\nu,\delta_{\rm in},T_2,\gamma_1,\Gamma_r) = 1$, the echo field $\hat{b}_o(t)$ reproduces completely the input light field with the same temporal shape and temporal order of the light pulses. Total photon number operator of the echo field signal irradiated at time $t > 2T_o + \tau_M$: $\hat{n}_e = \int_{-\infty}^{\infty}d\nu\hat{b}^\dagger_o(\nu)\hat{b}_o(\nu) = \sum_{k=1}^{M}\hat{n}_{e,k}$, where $\hat{n}_{e,k} = \gamma_1 e^{-4T_o/T_2}\int_\tau^\infty dt'\hat{a}^\dagger_{e,k}(t')\hat{a}_{e,k}(t')$ relates to the kth field mode with average photon number $\langle\hat{n}_{e,k}\rangle = e^{-4T_o/T_2}Q_{e,k}\bar{n}_{1,k}$ and

$$Q_{e,k} = \int_{-\infty}^{+\infty}d\nu[Z_r(\nu,\delta_{\rm in},T_2,\gamma_1,\Gamma_r)]^2\frac{\langle\hat{n}_{1,k}(\nu)\rangle}{\bar{n}_{1,k}}. \tag{29}$$

Finally by using Eqs. (28) and (29) and taking into account quantum efficiency $Q_{e,k}$ we can normalize output state $| < \psi_{{\rm out},k}(t-2T_o)|\psi_{{\rm out},k}(t-2T_o) > | \equiv 1$ for the input single photon wave packets $f_k(\nu)$, and then we obtain a fidelity $F_k = | < \psi_{{\rm in},k}(t)|\psi_{{\rm out},k}(t-2T_o) > |^2$ for the retrieved kth single photon input field. The fidelity is expressed via the spectral properties of the S function and input light field as

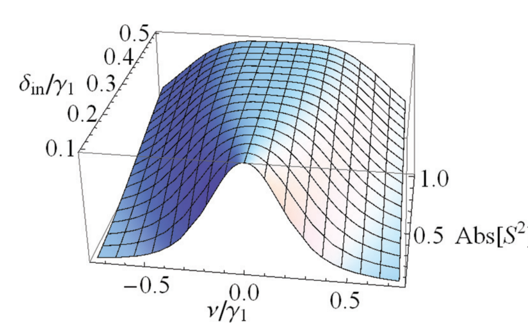

FIG. 8. (Color online) SS function for small inhomogeneous broadening $0.1 < \delta_{\rm in}/\gamma_1 < 0.5$ demonstrates perfect efficiency within spectral range $-0.25 < \nu/\gamma_1 < 0.25$ for inhomogeneous broadening width $\delta_{\rm in} \approx 0.5\gamma_1$.

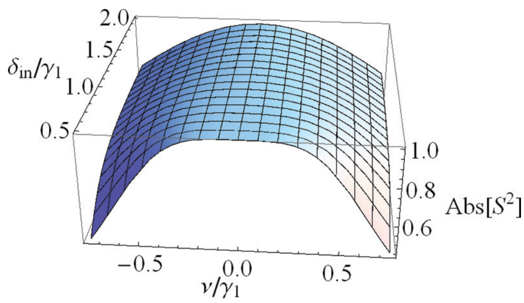

FIG. 9. (Color online) SS function for larger inhomogeneous broadening $\delta_{\rm in}$; we see transfer of quantum efficiency from the flat behavior within spectral range $-0.25 < \nu/\gamma_1 < 0.25$ to the quadratic spectral behavior for large inhomogeneous broadening $\delta_{\rm in}$: $\delta_{\rm in} \gg 0.5\gamma_1$.

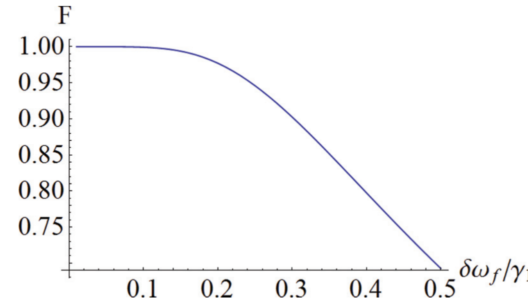

FIG. 11. (Color online) Fidelity of the echo field retrieval (30) for input light pulse with Gaussian spectral shape $\langle \hat{n}_{1,k}(\nu)\rangle \sim \frac{1}{\sqrt{2\pi}\delta\omega_f}\exp\{-\frac{\nu^2}{2\delta\omega_f^2}\}$ as a function of spectral width $\delta\omega_f$; fidelity decay for large spectral width of the input pulse $\delta\omega_f > 0.2\gamma_1$ is a result of the amplitude and phase modulation of the emitted echo field.

follows:

$$F_k = \frac{\left|\int_{-\infty}^{+\infty} d\nu [S_r(\nu,\delta_{\rm in},T_2,\gamma_1,\Gamma_r)]^2 |f_k(\nu)|^2\right|^2}{Q_{e,k}}. \quad (30)$$

By comparing the properties of echo field $\hat{b}_o(t)$ with the properties of echo field emitted in the time reversal CRIB scheme in the optimal optical cavity [20], we see the square of the S function $[S_r(\nu,\ldots)]^2 = Z_r(\nu,\ldots)\exp\{2i\varphi(\nu)\}$ demonstrates an additional amplitude and phase modulation of the echo field (28) while the CRIB protocol determines only the amplitude modulation of echo field spectral components proportionally to the SS function $Z_r(\nu,\delta_{\rm in},T_2,\gamma_1,\Gamma_r)$. Appearance of the additional phase modulation (the phase $|\varphi(\nu)|$ and imaginary part of the S function, respectively, increase with the spectral detuning $|\nu|$) is a result of loss of the complete temporal reversibility in the light atom dynamics related to the echo emission in comparison with the storage stage as demonstrated recently for standard broadband AFC protocol [14].

Figures 6 and 7 show spectral properties of the imaginary part for the square of the S function as function of IB width $\delta_{\rm in}$. It is seen that satisfying both matching conditions we get a significant phase modulation only for the echo fields excited by the input signal field with larger spectral width $\delta\omega_f > 0.25\delta_{\rm in}$. It is important the phase modulation does not effect the quantum efficiency of echo emission in opposite to the case of AFC protocol, since the quantum efficiency of echo irradiation (29) is determined by an SS function similar to the completely time-reversal CRIB scheme, and it is determined by the small optical depth of the atomic system. Moreover the additional phase modulations can be highly suppressed in the case of two matching conditions and narrow spectral width of the input signal fields where SS function $Z_r(\nu,\ldots)$ and S function $S_r(\nu,\ldots)$ will be both close to unity while the phase shift $\varphi(\nu)$ almost vanishes in this spectral range. Spectral properties of the SS function depicted in Figs. 8 and 9 show almost ideal quantum efficiency for spectral components of input light signal in the spectral range $-0.25\gamma_1 < \nu < 0.25\gamma_1$ if both matching conditions are satisfied. Also we note that the additional phase modulation can be even completely ignored for a storage of the polarization quantum states of light (polarization photonic qubits), since both polarization components will get the same phase modulation without any influence to the self-interference and the used encoding of polarization light states.

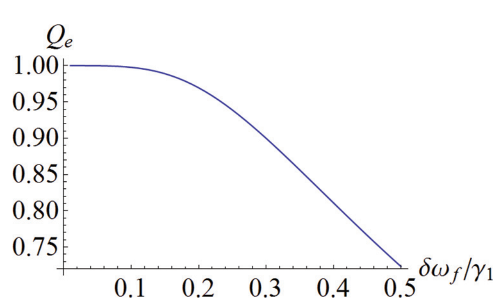

FIG. 10. (Color online) Quantum efficiency of the echo field retrieval (29) for input light pulse with Gaussian spectral shape $\langle \hat{n}_{1,k}(\nu)\rangle \sim \frac{1}{\sqrt{2\pi}\delta\omega_f}\exp\{-\frac{\nu^2}{2\delta\omega_f^2}\}$ as a function of spectral width $\delta\omega_f$.

Figures 10 and 11 demonstrate the quantum efficiency (29) and fidelity (30) for retrieval of the input light pulses with Gaussian spectral shape $\langle \hat{n}_{1,k}(\nu)\rangle \sim \frac{1}{\sqrt{2\pi}\delta\omega_f}\exp\{-\frac{\nu^2}{2\delta\omega_f^2}\}$ characterized by different spectral widths $\delta\omega_f$. As seen in the figures and in the solutions (3) and (28) we can implement a highly perfect retrieval of the input signal field with spectral width $\delta\omega_f < 0.2\gamma_1$ when the irradiated field will be only damped by the atomic decoherence for relatively large storage time $\hat{b}(t) = \exp\{-2T_o/T_2\}\sum_{k=1}^{M}\hat{b}_k(t-2T_o-\tau_k)$. Increasing the input signal light spectral width will lead to some spectral filtration and phase modulation in the echo field spectral components $|\nu| > 0.2\gamma_1$ resulting in appropriate decrease of the quantum efficiency and fidelity as depicted in Figs. 10 and 11 that can determine the optimal spectral parameters of the input signal light fields.

V. CONCLUSION

Thus a scheme of photon echo quantum memory based on the off-resonant Raman atomic transition in optimal optical QED cavity has been proposed. The scheme involves a number of unique advantages which all are critical for realization of fine robust coherent control of the interaction between the IB atomic systems and weak single photon fields. This scheme makes it possible to use the optically thin atomic systems with natural IB on the Raman transition, which can be characterized by arbitrary narrow homogeneous isochromatic groups of atoms as it occurs for the forbidden transition for rare-earth ions in inorganic crystals [4,24,32,36], NV centers in diamond [44,45], and other solid state systems [46,47]. It has been shown that the used optical cavity provides a fine control of the atomic ensembles by external laser fields propagating without any losses along transverse path to the optical cavity mode while a strong enhancement of the atomic interaction with the cavity mode field offers an easer experimental method for highly efficient quantum storage of rather arbitrary multimode light fields in the optical thin medium. Thus the scheme provides a number of experimental tools immune to many typical decoherent processes for a robust implementation of the practically realizable QM. The proposed optical QM can be easily implemented with well-known optical technique on various atomic ensembles in a broad spectral range of the light fields. In particular it can be also realized on the planar superconducting resonators with transverse coherent laser control of resonant atomic (spin) ensembles. This scheme is promising for the quantum repeaters based on the light-atom interface coupling microwave and optical photons and for the quantum RAM in superconducting quantum computer. All the mentioned properties indicate a great potential for using this technique in quantum repeaters and in quantum random access memory for quantum computers.

ACKNOWLEDGMENTS

The author would like to thank the Russian Foundation for Basic Research through Grant No. 12-02-91700 for partial financial support of this work.

[1] A. I. Lvovsky, B. C. Sanders, and W. Tittel, Nature Photonics **3**, 706 (2009).

[2] K. Hammerer, A. S. Sörensen, and E. S. Polzik, Rev. Mod. Phys. **82**, 1041 (2010).

[3] C. Simon *et al.*, Eur. Phys. J. D **58**, 1 (2010).

[4] W. Tittel *et al.*, Laser Phot. Rev. **4**, 244 (2010).

[5] J.-L. Le Gouët and S. A. Moiseev, J. Phys. B: Atom. Mol. Opt. Phys. **45**, 120201 (2012).

[6] S. A. Moiseev and S. Kröll, Phys. Rev. Lett. **87**, 173601 (2001).

[7] M. P. Hedges *et al.*, Nature (London) **465**, 1052 (2010).

[8] M. Hosseini, B. M. Sparkes, P. Lam, and B. Buchler, Nature Commun. **2**, 174 (2011); M. Hosseini *et al.*, J. Phys. B: Atom. Mol. Opt. Phys. **45**, 134004 (2012).

[9] H. De Riedmatten *et al.*, Nature (London) **456**, 773 (2008).

[10] C. Clausen *et al.*, Nature (London) **469**, 508 (2011).

[11] E. Saglamyurek *et al.*, Nature (London) **469**, 512 (2011).

[12] I. Usmani *et al.*, Nat. Commun. **1**, 1 (2010).

[13] M. Bonarota, J.-L. Le Gouët, and T. Chaneliere, New J. Phys **13**, 013013 (2011).

[14] S. A. Moiseev and J.-L. Le Gouët, J. Phys. B: Atom. Mol. Opt. Phys. **45**, 124003 (2012).

[15] M. Bonarota, J.-L. Le Gouët, S. A. Moiseev, and T. Chanelière, J. Phys. B: Atom. Mol. Opt. Phys. **45**, 124002 (2012).

[16] S. A. Moiseev, Phys. Rev. A **83**, 012307 (2011).

[17] D. L. McAuslan, P. M. Ledingham, W. R. Naylor, S. E. Beavan, M. P. Hedges, M. J. Sellars, and J. J. Longdell, Phys. Rev. A **84**, 022309 (2011).

[18] V. Damon *et al.*, New J. Phys. **13**, 093031 (2011).

[19] B. S. Ham, Phys. Rev. A **85**, 031402(R) (2012).

[20] S. A. Moiseev, S. N. Andrianov, and F. F. Gubaidullin, Phys. Rev. A **82**, 022311 (2010); S. A. Moiseev and S. N. Andrianov, J. Phys. B: Atom. Mol. Opt. Phys. **45**, 124017 (2012).

[21] S. A. Moiseev and M. I. Noskov, Laser Phys. Lett. **1**, 303 (2004).

[22] B. Kraus, W. Tittel, N. Gisin, M. Nilsson, S. Kroll, and J. I. Cirac, Phys. Rev. A **73**, 020302 (2006).

[23] M. Afzelius and C. Simon, Phys. Rev. A **82**, 022310 (2010).

[24] M. Sabooni, S. T. Kometa, A. Thuresson, S. Kröll, and L. Rippe, New J. Phys. **15**, 035025 (2013); M. Sabooni, Q. Li, S. Kröll, and L. Rippe, Phys. Rev. Lett. **110**, 133604 (2013).

[25] S. A. Moiseev and W. Tittel, New J. Phys. **13**, 063035 (2011).

[26] J. Nunn, K. Reim, K. C. Lee, V. O. Lorenz, B. J. Sussman, I. A. Walmsley, and D. Jaksch, Phys. Rev. Lett. **101**, 260502 (2008).

[27] J. L. Le Gouët and P. R. Berman, Phys. Rev. A **80**, 012320 (2009).

[28] E. S. Moiseev and S. A. Moiseev, arXiv:1301.0499v2 [quant-ph].

[29] D. F. Walls and G. J. Milburn, *Quantum Optics* (Springer, Heidelberg, 1994).

[30] M. Tavis and F. W. Cummings, Phys. Rev. **170**, 379 (1968).

[31] M. O. Scully and S. M. Zubairy, *Quantum Optics* (Cambridge University Press, Cambridge, 1997).

[32] K. Ichimura and H. Goto, Phys. Rev. A **74**, 033818 (2006).

[33] J. R. Buck and H. J. Kimble, Phys. Rev. A **67**, 033806 (2003).

[34] H. A. Haus, *Waves and Fields in Optoelectronics* (Prentice-Hall, Englewood Cliffs, NJ, 1984).

[35] A. E. Siegman, *Lasers* (University Science Books, Mill Valley, CA, 1986).

[36] B. S. Ham, P. R. Hemmer, and M. S. Shahriar, Opt. Comm. **144**, 227 (1997).

[37] D. L. McAuslan, J. J. Longdell, and M. J. Sellars, Phys. Rev. A **80**, 062307 (2009).

[38] R. H. Dicke, Phys. Rev. **93**, 99 (1954).

[39] L. Allen and J. H. Eberly, *Optical Resonance and Two-Level Atoms* (Wiley, New York, 1975).

[40] S. A. Moiseev, Opt. Spectrosc. **62**, 180 (1987).

[41] S. A. Moiseev, Izv. Ross. Akad. Nauk, Ser. Fiz. **68**, 1260 (2004) [Bull. Russ. Acad. Sci. Phys. **68**, 1408 (2004)].

[42] G. L. Lamb, Jr., *Elements of Soliton Theory* (Wiley, New York, 1980).

[43] V. I. Rupasov, Zh. Eksp. Teor. Fiz. **83**, 1711 (1982) [Sov. Phys. JETP **56**, 989 (1982)].

[44] G. Balasubramanian *et al.*, Nat. Mater. **8**, 383 (2009).

[45] P. C. Maurer *et al.*, Science **336**, 1283 (2012).

[46] A. M. Tyryshkin *et al.*, Nat. Mater. **11**, 143 (2011).

[47] M. Steger *et al.*, Science **336**, 1280 (2012).